

Two-pulse photon echo electron-nuclear double resonance of  $\text{YAlO}_3\text{:Pr}^{3+}$ 

R. M. Shelby and R. M. Macfarlane  
*IBM Research Laboratory, San Jose, California 95193*

R. L. Shoemaker  
*Optical Sciences Center, University of Arizona, Tucson, Arizona 85721*  
 (Received 25 January 1982)

Two-pulse photon echo electron-nuclear double resonance (or PENDOR) has been used to measure the second-order hyperfine splittings in the ground state and the lowest component of the excited  $^1D_2$  state of  $\text{YAlO}_3\text{:Pr}^{3+}$ . The excited-state splittings are 0.923 and 1.565 MHz and are significantly different from previous hole-burning results because of greatly increased resolution. The mechanism for two-pulse PENDOR involves a modulation of the photon echo decay at the rf Rabi frequency. This modulation has been observed directly. A brief theoretical analysis is given which shows that the echo modulation is a result of phase and amplitude changes in the oscillating optical dipole moment which are indirectly produced by the rf field.

## I. INTRODUCTION

Optical-rf double resonance is a very useful technique for the study of hyperfine interactions in solids, since it offers resolution limited by the rf source together with the high sensitivity characteristic of optical measurements. Thus, it can be a useful supplement to optical hole burning, when the hyperfine splittings become comparable to the laser frequency stability. The technique of electron-spin echo electron-nuclear double resonance (ENDOR) was originally developed by Mims<sup>1</sup> and was extended to the optical region by Hartmann and collaborators<sup>2</sup> as photon echo nuclear double resonance (PENDOR). In all these experiments the amplitude of a three-pulse stimulated echo was reduced by the application of a resonant rf pulse between the second and third pulses of the echo sequence. The rf resonance can be with either the levels of neighboring nuclei<sup>1,2</sup> or in the case of photon echoes, the nuclear hyperfine levels of the optical center itself. The decay of the stimulated echo is controlled by population changes ( $T_1$  processes) and spectral diffusion, and the application of resonant rf alters the echo amplitude by inducing additional population changes in the case of hyperfine levels or by altering the local fields at optical centers in the case of transitions of neighboring nuclei.<sup>1-3</sup> Chiang *et al.*<sup>4</sup> recently used this technique to measure the hyperfine splittings of the lowest component of the  $^1D_2$  excited state of  $\text{LaF}_3\text{:Pr}^{3+}$  and found values of 3.7 and 4.65 MHz, in agreement with optical hole burning.<sup>5</sup>

We have carried out PENDOR experiments using an experimental arrangement that differs somewhat from that used previously.<sup>1-4</sup> We observe the ampli-

tude of a two-pulse photon echo while simultaneously irradiating nuclear levels with rf, and the effect of the rf on the echo is to modulate its decay at the rf Rabi frequency. This modulation effect has also been observed directly and is reported below. We chose to study the hyperfine splittings of the lowest  $^1D_2$  level of  $\text{YAlO}_3\text{:Pr}^{3+}$  because the splittings are small ( $\sim 1$  MHz) and poorly resolved in optical hole-burning experiments.<sup>6</sup> The increased resolution of the PENDOR technique gives well-resolved splittings, enabling them to be much more accurately measured. In these experiments, individual hyperfine levels were excited by using an amplitude-gated single-frequency cw dye laser, and the hyperfine splittings measured by scanning an external rf frequency. An alternative method of measuring these splittings is to study echo modulation as a function of pulse separation using short pulses whose Fourier width is greater than the hyperfine splittings.<sup>7</sup> Although the hyperfine splittings can often be extracted from the complicated modulation patterns by Fourier transformation, the interpretation of these experiments is not straightforward.<sup>4</sup>

## II. RESULTS

Two-pulse photon echoes were measured on the 6107-Å transition of a 0.1%  $\text{YAlO}_3\text{:Pr}^{3+}$  crystal at 1.7 K as previously described.<sup>8</sup> The echo decay time ( $T_2$ ) was 35  $\mu\text{sec}$ . The separation between the  $\pi$  and  $\frac{1}{2}\pi$  pulses was set to be  $\tau = 20 \mu\text{sec}$  and rf pulses of  $\sim 50\text{-}\mu\text{sec}$  duration were applied as shown in Fig. 1. This value of  $\tau$  is short enough that significant echo amplitude is available for the double-

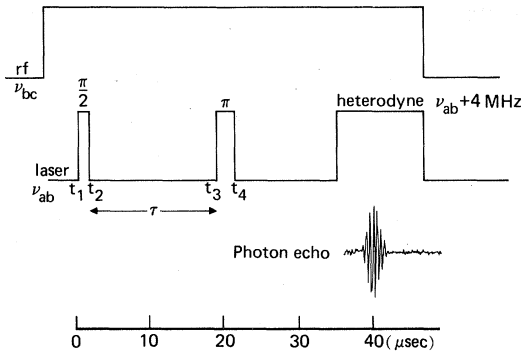


FIG. 1. rf and optical pulse sequence used for observation of two-pulse PENDOR. The frequency of the heterodyne pulse is shifted by 4 MHz from the excitation frequency.

resonance experiment but long enough to obtain changes in amplitude of 20%–50% with small rf field strengths (typically  $\sim 0.5$  G), thus minimizing power broadening. The rf frequency was stepped in increments of 5–10 kHz and the echo amplitude measured using a transient digitizer.

The resulting spectrum is shown in Fig. 2. The two resonances near 1 MHz are the hyperfine transitions within the lowest component of the  $^1D_2$  excited state. The values we obtain are 0.923 and 1.565 MHz, which are significantly different from those obtained from hole burning,<sup>6</sup> i.e., 1.065 and 1.416 MHz. The discrepancy seems to arise from uncer-

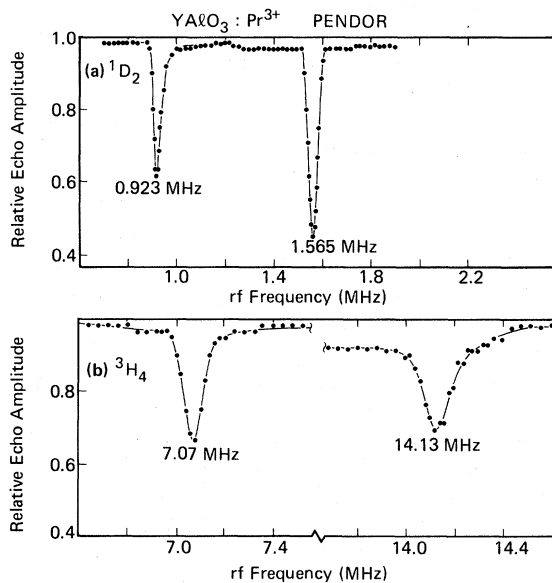


FIG. 2. PENDOR signals observed in 0.1%  $\text{YAlO}_3:\text{Pr}^{3+}$  at 1.6 K with  $\tau = 20 \mu\text{sec}$ . (a) The lowest component of the  $^1D_2$  excited state at 6107 Å. The two transitions are those allowed between the quadrupole levels of  $I = \frac{5}{2}$ . (b) The same but for the ground state.

tainties in the deconvolution of the laser frequency jitter limited hole and antihole pattern which was required in the hole burning work. Both excited-state and ground-state hyperfine resonances can be detected via PENDOR. The ground-state resonance frequencies we obtained (7.07 and 14.13 MHz) agree with the results of optically detected NQR,<sup>6</sup> i.e., 7.049 and 14.124 MHz. The second-order hyperfine interaction in the excited state is much less than in the ground state,<sup>6</sup> and hence, as expected, the PENDOR linewidths in the excited state are smaller (see Fig. 2).

### III. THEORY AND DISCUSSION

In our experiment the PENDOR signal has its origin in a modulation of the echo amplitude as a function of  $\tau$  due to rf nutation of the nuclear spins. The rf induced Rabi flopping of the spins indirectly changes the phase and amplitude of the oscillating optical dipole moment and thereby changes the photon echo amplitude. This is unlike previous stimulated echo PENDOR experiments where the echo amplitude is directly proportional to the population of one of the rf-coupled levels. We have carried out a theoretical analysis of this three-level problem (see Fig. 3) by solving the density matrix equations of motion using the following simplifying assumptions:

(i) Only one three-level system is resonant at any one time. This is always satisfied since the laser width and the optical and rf nutation frequencies are less than the hyperfine splittings.

(ii) The photon echo excitation pulses are exactly  $\frac{1}{2}\pi$  and  $\pi$  pulses and all ions within the inhom-

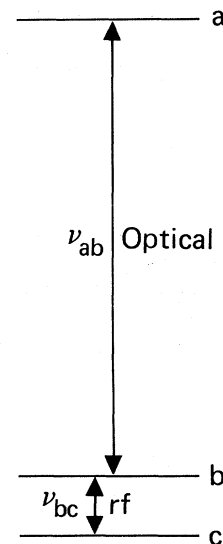


FIG. 3. Three-level model for two-pulse PENDOR theory.

geneous line are assumed to interact resonantly. Although this condition is not fulfilled in our experiments, only the absolute magnitude of the echo and its detailed shape is changed by different pulse areas and off-resonance excitation. The essentials of the echo modulation are not affected by this simplifying approximation.

(iii) During the optical pulses, excitation by the rf field and all relaxation is ignored. This is a good approximation since the optical pulses are much shorter than the relaxation times and  $\omega_1^{-1}$  where  $\omega_1$  is the resonant rf Rabi frequency.

(iv) The level decay rates  $\gamma_{aa}$ ,  $\gamma_{bb}$ ,  $\gamma_{cc}$  are very small and can be ignored. (In  $\text{YAlO}_3:\text{Pr}^{3+}$ ,  $\gamma_{aa} \sim 5 \times 10^3 \text{ sec}^{-1}$ , and  $\gamma_{bb}, \gamma_{cc} \approx 0.1 \text{ sec}^{-1}$ .) The dephasing rates  $\gamma_{ab}$ ,  $\gamma_{ac}$  are much faster and are included ( $\gamma_{ab} \approx \gamma_{ac} = 3 \times 10^4 \text{ sec}^{-1}$ ). The value of  $\gamma_{bc}$  is irrelevant as it does not enter the echo expression.

With these assumptions the system can be considered to be subjected to only one field at any given time and the equations of motion separate into two sets of coupled equations. One set just describes the ordinary two-level system in the presence of the relevant driving field (light or rf). The other set describes the coherence between the third-level and this two-level system. The solutions obtained for different time intervals are then combined as detailed in the Appendix. The final result is that the peak amplitude of the heterodyne-detected echo at time  $t_4 + \tau$  is given by  $A_{\text{peak}}$ :

$$A_{\text{peak}} = \frac{1}{4} e^{-2\gamma\tau} (N_b - N_a) \times [(1 + \delta^2/g^2) + (1 - \delta^2/g^2) \cos g\tau] \quad (1)$$

where  $\delta$  is the rf frequency detuning from resonance with the  $b \leftrightarrow c$  transition,  $g = (\delta^2 + \omega_1^2)^{1/2}$ ,  $(N_b - N_a) \approx N_b$  is the population difference between optical levels, and  $\tau = t_3 - t_2$ .

We first consider the echo modulation that occurs for a strong, resonant rf field (i.e.,  $\delta = 0$ ). Then

$$A_{\text{peak}} = \frac{1}{4} e^{-2\gamma\tau} (N_b - N_a) (1 + \cos \omega_1 \tau) \quad (2)$$

This gives a damped oscillatory echo decay with damping constant  $T_2 = \gamma^{-1}$  and oscillation period  $2\pi/\omega_1$ . To demonstrate this modulation effect we irradiated the  $\text{Pr}^{3+}$  ground-state transition at 7.05 MHz such that the Rabi frequency was much greater than the optical homogeneous linewidth (9 kHz). The Rabi frequency of  $\omega_1/2\pi = 108 \text{ kHz}$  was measured directly by optical detection of the rf nutation.<sup>9</sup> The photon echo decay was modulated as shown in Fig. 4. The modulation frequency is in agreement with the prediction of Eq. (2), but the depth of modulation is not 100%. This is because of echo signals originating from hyperfine levels which are not coupled by rf, and to the fact that the rf transition is inhomogeneously broadened.

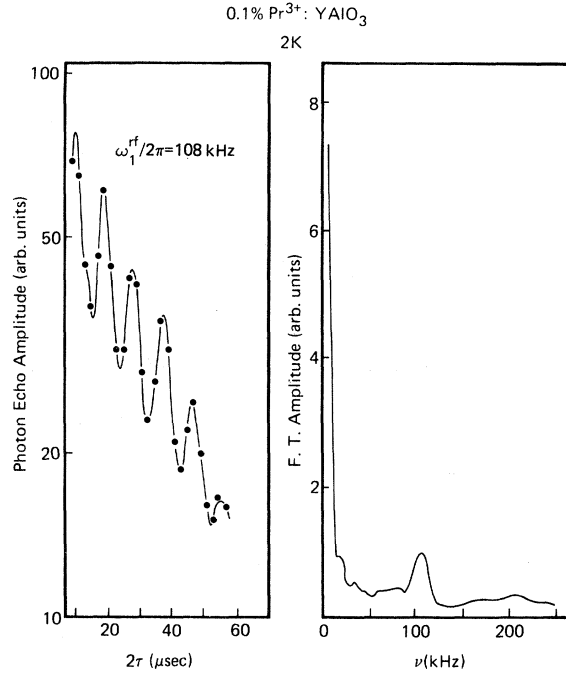


FIG. 4. (a) Photon echo modulation observed during the application of rf at the 7.07-MHz ground-state resonance. For the rf field strength used, the nuclear Rabi frequency was 108 kHz. (b) Fourier transform of the echo decay in (a) showing the frequency splitting induced by rf irradiation.

The results shown in Eqs. (1) and (2) were calculated using a semiclassical density matrix treatment. An alternative way of looking at the effect is to say that the rf field puts "Rabi sidebands" on the optical transition and the  $\sim 1\text{-}\mu\text{sec}$  laser pulses prepare a superposition of these dressed states. The modulated echo can then be regarded as simply resulting from the simultaneous excitation of several coupled levels. Echo modulation of this kind has previously been used by Chen *et al.* to measure hyperfine splittings.<sup>7</sup> These high-frequency modulations are not observed here because of our selective (long pulse) excitation, which does not allow a superposition of hyperfine states to be excited. Instead our technique allows very small splittings to be measured with resolution limited not by optical inhomogeneous broadening, but only by inhomogeneous broadening of the small splitting itself. The Fourier transform of the echo decay shown in Fig. 4 demonstrates this by showing the sideband produced by the rf Rabi frequency.

To analyze the PENDOR resonance we note that Eq. (1) expresses the echo signal as the rf field is scanned through resonance with  $\omega_{bc}$ , i.e., as  $\delta$  is varied. For sufficiently strong rf, the factor in square brackets varies between a maximum of 2 and minimum of 0. Figure 5 shows a plot of Eq. (1) for  $\omega_1\tau = 1.6$  and  $\omega_1/2\pi = 13 \text{ kHz}$ . Under these condi-

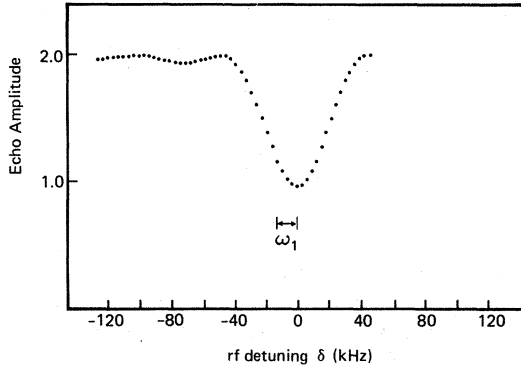


FIG. 5. Echo amplitude as a function of rf detuning calculated from Eq. (1) with  $\omega_1\tau = 1.6$  and  $\omega_1/2\pi = 13$  kHz.

tions of  $\sim 50\%$  reduction in echo signal, the power broadening is  $\sim 3\omega_1$ . Although the qualitative picture provided by the theory is in good agreement with experiment, a detailed correspondence cannot be expected since the experimental linewidth is mostly determined by inhomogeneous broadening of the nuclear hyperfine transitions.

#### IV. CONCLUSION

In conclusion, we have used two-pulse PENDOR to measure the hyperfine splittings in the ground  $^3H_4$  state and the lowest crystal-field component of the excited  $^1D_2$  state of  $\text{YAIO}_3\text{:Pr}^{3+}$ . The accuracy of determining the excited-state splittings is much greater than could be obtained by optical hole burning, so much improved values are obtained. The PENDOR signal arises from an echo modulation due to rf nutation of the hyperfine levels and this modulation is demonstrated experimentally. A theoretical analysis of two-pulse PENDOR is given, using a number of simplifying but realistic assumptions, and the results are consistent with experimental observations.

#### ACKNOWLEDGMENTS

We wish to thank D. P. Burum for a number of helpful discussions and one of us (R.L.S.) gratefully

acknowledges the support of the National Science Foundation under Grant No. CHE-7824085.

#### APPENDIX

To work out a theory for two-pulse photon echo ENDOR in the three-level system of Fig. 1(b), we need solutions for the density matrix equations of motion in two situations: during the two optical pulses, and between the pulses. Consider first the situation between the pulses, when only the rf field  $H_1 \cos\omega_{\text{rf}}t$  is present. We then have

$$\dot{\rho}_{aa} = 0, \quad (\text{A1a})$$

$$\dot{\rho}_{cc} - \dot{\rho}_{bb} = 2i(\rho_{bc} - \rho_{bc}^*)\kappa H_1 \cos\omega_{\text{rf}}t, \quad (\text{A1b})$$

$$\dot{\rho}_{bc} = -(i\omega_{bc} + \gamma_{bc})\rho_{bc} + (\rho_{cc} - \rho_{bb})i\kappa H_1 \cos\omega_{\text{rf}}t, \quad (\text{A1c})$$

$$\dot{\rho}_{ab} = -(i\omega_{ab} + \gamma)\rho_{ab} - (i\kappa H_1 \cos\omega_{\text{rf}}t)\rho_{ac}, \quad (\text{A1d})$$

$$\dot{\rho}_{ac} = -(i\omega_{ac} + \gamma)\rho_{ac} - (i\kappa H_1 \cos\omega_{\text{rf}}t)\rho_{ab}, \quad (\text{A1e})$$

where the coupling constant  $\kappa = \mu_N g_N / 2\hbar$  with  $\mu_N$  being the nuclear magneton and  $g_N$  the nuclear  $g$  value for the  $b \leftrightarrow c$  transition. As explained in the text, we are ignoring the slow level-decay and pumping processes and have assumed equal dephasing rates  $\gamma_{ab} = \gamma_{ac} = \gamma$ .

We now note that these three equations break-up into two independent pairs of equations. Equations (A1b) and (A1c) are just the usual equations for a two-level system (when pumping and level decay rates are ignored). Their solution in various limits is well known, but is not needed for the problem at hand.

The second pair of equations, (A1d) and (A1e), are of primary interest because  $\rho_{ab}$  is the quantity that gives rise to the echo. These equations may be solved by setting

$$\begin{aligned} \rho_{ab} &= \tilde{\rho}_{ab} \exp[-(i\omega_{ab} + \gamma)t], \\ \rho_{ac} &= \tilde{\rho}_{ac} \exp[-(i\omega_{ac} + \gamma)t]. \end{aligned} \quad (\text{A2})$$

One then finds

$$\begin{aligned} \rho_{ab}(t_{n+1}) &= \frac{1}{g} \{ -i\kappa H_1 \rho_{ac}(t_n) e^{i\omega_{ac}t_n} \sin(gt'/2) \\ &\quad + \rho_{ab}(t_n) e^{i\omega_{ab}t_n} [g \cos(gt'/2) + i\delta \sin(gt'/2)] \} e^{i\delta t'/2} e^{-\gamma t'} \exp(-i\omega_{ab}t_{n+1}), \\ \rho_{ac}(t_{n+1}) &= \frac{1}{g} \{ \rho_{ac}(t_n) e^{i\omega_{ac}t_n} [g \cos(gt'/2) - i\delta \sin(gt'/2)] \\ &\quad - i\kappa H_1 \rho_{ab}(t_n) e^{i\omega_{ab}t_n} \sin(gt'/2) \} e^{i\delta t'/2} e^{-\gamma t'} \exp(-i\omega_{ac}t_{n+1}) \end{aligned} \quad (\text{A3})$$

for a time period beginning at time  $t_n$  and ending at time  $t_{n+1}$ . Here  $t' = t_{n+1} - t_n$ ,  $\delta = \omega_{bc} - \omega_{rf}$  is the detuning of the rf field from resonance, and  $g = [\delta^2 + (\omega_1)^2]^{1/2}$  is the rf Rabi flopping frequency, where  $\omega_1 = \kappa H_1$ .

During the optical pulse, a different set of density matrix equations is needed, namely,

$$\dot{\rho}_{cc} = 0, \quad (\text{A4a})$$

$$\dot{\rho}_{bb} - \dot{\rho}_{aa} = 2i(\rho_{ab} - \rho_{ab}^*)\kappa_0 E_0 \cos \Omega t, \quad (\text{A4b})$$

$$\dot{\rho}_{ab} = -i\omega_{ab}\rho_{ab} + (\rho_{bb} - \rho_{aa})i\kappa_0 E_0 \cos \Omega t, \quad (\text{A4c})$$

$$\dot{\rho}_{ac} = -i\omega_{ac}\rho_{ac} + (i\kappa_0 E_0 \cos \Omega t)\rho_{bc}, \quad (\text{A4d})$$

$$\dot{\rho}_{bc} = -i\omega_{bc}\rho_{bc} + (i\kappa_0 E_0 \cos \Omega t)\rho_{ac}, \quad (\text{A4e})$$

where the coupling constant is  $\kappa_0 = P_{ab}/\hbar$  with  $P_{ab}$  being the transition dipole matrix element, and  $E_0 \cos \Omega t$  is the applied optical field during the pulse.

Again we have two independent pairs of equations. Equations (A4b) and (A4c) are equivalent to the standard undamped optical Bloch equations. Assuming the pulse is very short so that all ions interact resonantly, these have the solution

$$\rho_{ab}(t_{n+1}) = \frac{1}{2} \{ \rho_{ab}(t_n) (1 + \cos \kappa_0 E_0 t') e^{i\Omega t_n} + \rho_{ab}^*(t_n) (1 - \cos \kappa_0 E_0 t') e^{-i\Omega t_n} + i[\rho_{bb}(t_n) - \rho_{aa}(t_n)] \sin \kappa_0 E_0 t' \} e^{-i\Omega t_{n+1}}, \quad (\text{A5})$$

$$\rho_{bb}(t_{n+1}) - \rho_{aa}(t_{n+1}) = i[\rho_{ab}(t_n) e^{i\Omega t_n} - \rho_{ab}^*(t_n) e^{-i\Omega t_n}] \sin \kappa_0 E_0 t' + [\rho_{bb}(t_n) - \rho_{aa}(t_n)] \cos \kappa_0 E_0 t',$$

for a pulse which begins at time  $t_n$  and ends at time  $t_{n+1}$ . As before,  $t' = t_{n+1} - t_n$ .

The second pair of equations, (A4d) and (A4e), are identical in form to Eqs. (A1d) and (A1e). The solutions are simpler, however, because we are assuming exact resonance ( $\Omega = \omega_{ab}$ ). One finds

$$\rho_{bc}(t_{n+1}) = [\rho_{bc}(t_n) e^{i\omega_{bc} t_n} \cos(\kappa_0 E_0 t'/2) + i\rho_{ac}(t_n) e^{i\omega_{ac} t_n} \sin(\kappa_0 E_0 t'/2)] \exp(-i\omega_{bc} t_{n+1}), \quad (\text{A6})$$

$$\rho_{ac}(t_{n+1}) = [i\rho_{bc}(t_n) e^{i\omega_{bc} t_n} \sin(\kappa_0 E_0 t'/2) + \rho_{ac}(t_n) e^{i\omega_{ac} t_n} \cos(\kappa_0 E_0 t'/2)] \exp(-i\omega_{ac} t_{n+1}).$$

We are now in a position to calculate the photon echo signal. First of all, we note that the echo in our experiments is detected as a heterodyne beat between a frequency shifted optical field  $E_h \cos(\Omega + \Delta)t$  and the field  $\epsilon_c \cos \Omega t$  emitted by the ions during the echo. Thus, the observed signal at the detector is

$$I(t) = \frac{1}{2} c \epsilon_0 (E_h^2 + E_h \epsilon_c \cos \Delta t) = I_h - \hbar \Omega L \kappa_0 E_h \left[ \int_{-\infty}^{\infty} \text{Im}[\rho_{ab}(t) e^{i\Omega t}] d\omega_{ab} \right] \cos \Delta t, \quad (\text{A7})$$

where  $L$  is the length of the sample. We note that although there is also a large nonzero density matrix element  $\rho_{ac}$ , the selection rules in  $\text{YAlO}_3:\text{Pr}^{3+}$  cause the transition dipole matrix element  $\rho_{ac}$  to be small. Thus, the contribution of  $\rho_{ac}$  to  $\epsilon_c$  can be ignored.

The calculation of  $\rho_{ab}(t)$  is straightforward, but tedious. We begin at time  $t_1$  (see Fig. 1) with the system in thermal equilibrium so that  $\rho_{ab}(t_1) = \rho_{ac}(t_1) = \rho_{bc}(t_1) = 0$  and  $\rho_{aa}(t_1) = n_a$ ,  $\rho_{bb}(t_1) = n_b$ ,  $\rho_{cc}(t_1) = n_c$ , where  $n_a, n_b, n_c$  are the thermal equilibrium populations in levels  $a, b, c$  for a group of ions which all experience the same local field and thus have the same resonance frequencies. We can then use Eqs. (A5) and (A6) with the  $\rho_{ij}(t_1)$  as initial conditions and  $\kappa_0 E_0(t_2 - t_1) = \frac{1}{2}\pi$  to find  $\rho_{ij}(t_2)$ . These in turn can be used as initial conditions in Eqs. (A3) to find  $\rho_{ab}(t_3)$  and  $\rho_{ac}(t_3)$ . These are the only

two density matrix elements we need because the second pulse is a  $\pi$  pulse [ $\kappa_0 E_0(t_4 - t_3) = \pi$ ] which gives [using Eqs. (A5) and (A6)],

$$\rho_{ab}(t_4) = \rho_{ab}^*(t_3) \exp[-i\Omega(t_3 + t_4)], \quad (\text{A8})$$

$$\rho_{ac}(t_4) = -\rho_{ac}(t_3) \exp[-i\omega_{ac}(t_4 - t_3)].$$

Knowledge of just  $\rho_{ac}(t_4)$  and  $\rho_{ab}(t_4)$  is sufficient because the echo arises only from  $\text{Im}(\rho_{ab})$  during the time interval  $t > t_4$ , and according to Eqs. (A3),  $\rho_{ab}$  is coupled only to  $\rho_{ac}$  during this period. In reality, we do not even need to know  $\rho_{ac}(t_4)$  or assume a  $\pi$  pulse, because one can show that a photon echo can only arise from the term  $\rho_{ab}^*(t_3)(1 - \cos \kappa_0 E_0 t')$  in Eqs. (A5) no matter what pulse area is used.

Retaining the  $\frac{1}{2}\pi$ ,  $\pi$  pulse assumption for algebraic simplicity, we find

$$\rho_{ab}(t) = -\frac{1}{2g^2} (n_b - n_a) [\delta \sin(g\tau/2) + ig \cos(g\tau/2)] \{ g \cos[g(t - t_4)/2] + i\delta \sin[g(t - t_4)/2] \} \times \exp[-i\delta(t - t_4 - \tau)] \exp[-\gamma(t - t_4 + \tau)] \exp[i(\Omega - \omega_{ab})(t - t_4 - \tau)] e^{-i\Omega t}. \quad (\text{A9})$$

Here we have dropped the term proportional to  $\rho_{ab}(t_4)$  because it has an exponential dependence  $\exp[i(\Omega - \omega_{ab})(t - t_2)]$  and thus does not produce an echo. It is only a free-induction decay term.

On taking the imaginary part of  $\rho_{ab}(t) \exp(i\Omega t)$  from Eq. (A9), and substituting into Eq. (A7), we find for the observed signal

$$I(t) = I_h + \frac{1}{4}(N_b - N_a) \exp[-\Delta\omega^2(t - t_4 - \tau)^2/4] \exp[-\gamma(t - t_4 + \tau)] \\ \times ((2\delta/g) \sin[g(t - t_4 - \tau)/2] \sin[\delta(t - t_4 - \tau)/2] \\ + \{(1 + \delta^2/g^2) \cos[g(t - t_4 - \tau)/2] + (1 - \delta^2/g^2) \cos[g(t - t_4 + \tau)/2]\} \cos[\delta(t - t_4 - \tau)/2]) \quad (\text{A10})$$

Here we have assumed an inhomogeneous distribution of  $\omega_{ab}$ 's given by

$$n_b - n_a = \frac{1}{\Delta\omega\sqrt{\pi}}(N_b - N_a) \\ \times \exp[-(\Omega - \omega_{ab})^2/\Delta\omega^2] \quad (\text{A11})$$

where  $\Delta\omega$  is the half-width of the distribution and  $N_a, N_b$  are the total populations in levels  $a$  and  $b$ .

The peak echo amplitude occurs at  $t - t_4 = \tau$ , where Eq. (A10) simplifies to

$$I(t - t_4 = \tau) = I_h + \frac{1}{4}(N_b - N_a) e^{-2\gamma\tau} \\ \times [(1 + \delta^2/g^2) + (1 - \delta^2/g^2) \cos g\tau] \quad (\text{A12})$$

which is the result presented in the text as Eq. (1).

<sup>1</sup>W. B. Mims, Proc. R. Soc. London **283**, 452 (1965).

<sup>2</sup>P. Hu, R. Leigh, and S. R. Hartmann, Phys. Lett. **40A**, 164 (1972); P. F. Liao, P. Hu, R. Leigh, and S. R. Hartmann, Phys. Rev. A **9**, 332 (1974).

<sup>3</sup>M. Emschwiller, E. L. Hahn, and D. Kaplan, Phys. Rev. **118**, 414 (1960).

<sup>4</sup>K. Chiang, E. A. Whittaker, and S. R. Hartmann, Phys. Rev. B **23**, 6142 (1981).

<sup>5</sup>L. E. Erickson, Phys. Rev. B **16**, 4731 (1977).

<sup>6</sup>L. E. Erickson, Phys. Rev. B **19**, 4412 (1979).

<sup>7</sup>Y. C. Chen, K. Chiang, and S. R. Hartmann, Phys. Rev. B **21**, 40 (1980).

<sup>8</sup>R. M. Macfarlane, R. M. Shelby, and R. L. Shoemaker, Phys. Rev. Lett. **43**, 1726 (1979).

<sup>9</sup>R. M. Shelby, C. S. Yannoni, and R. M. Macfarlane, Phys. Rev. Lett. **41**, 1739 (1978).